JOURNAL OF MAGNETIC RESONANCE **133,** 388–394 (1998)
ARTICLE NO. MN981460

A Definitive Example of Aluminum-27 Chemical Shielding Anisotropy

Robert W. Schurko, Roderick E. Wasylishen,[1] and Andrew D. Phillips

Department of Chemistry, Dalhousie University, Halifax, Nova Scotia, Canada, B3H 4J3

Received November 12, 1997

Solid-state ^{27}Al NMR spectra have been obtained for a crystalline 1:1 complex of $AlCl_3$ and $OPCl_3$. Aluminum chloride phosphoryl chloride, $AlCl_3 \cdot OPCl_3$ (1), is unusual in that the Al–O–P bond angle is close to 180°. From analysis of the ^{27}Al MAS NMR spectra, it was determined that the ^{27}Al nuclear quadrupole coupling constant is 6.0(1) MHz, the asymmetry in the electric field gradient (efg) tensor is 0.15(2), and the isotropic chemical shift, $\delta_{iso}(^{27}Al)$, is 88(1) ppm. Solid-state ^{27}Al NMR of a stationary sample reveals a line shape affected by a combination of anisotropic chemical shielding and second-order quadrupolar interactions. Analysis of this spectrum yields a chemical shift anisotropy of 60(1) ppm and orientations of the chemical shift and electric field gradient tensors in the molecular frame. Experimental results are compared with those calculated using *ab initio* Hartree–Fock and density functional theory. © 1998 Academic Press

Key Words: **solid-state NMR; aluminum-27 NMR; chemical shift anisotropy; nuclear quadrupole coupling constants; *ab initio* chemical shielding tensors.**

INTRODUCTION

Solid-state aluminum-27 NMR is now routinely used for the characterization of many solid materials, including zeolites, gels, minerals, clays, metal alloys, amorphous solids, and numerous coordination compounds (*1–5*). Although ^{27}Al is a quadrupolar nucleus, spin $I = 5/2$, high-resolution NMR studies are feasible because ^{27}Al has a relatively small nuclear quadrupole moment ($Q = 0.14 \times 10^{-28}$ m^2) (*6*). Thus, in the moderate to high applied magnetic fields currently used by NMR spectroscopists, the central ^{27}Al NMR transition is generally only broadened by the second-order quadrupolar interaction, making the analysis of such high-resolution NMR spectra straightforward. The range of isotropic ^{27}Al chemical shifts is approximately 300 ppm (*7*); consequently, it is expected that ^{27}Al chemical shifts may be orientation dependent in some environments. In the majority of published solid-state ^{27}Al NMR studies, isotropic chemical shifts have been reported and in some cases, the effects of the nuclear quadrupole interaction on the ^{27}Al line shape have been simulated. Although many isotropic ^{27}Al chemical shifts have been reported in the literature in both the solid and liquid states (*2, 7*), there have been few definitive reports of ^{27}Al chemical shift anisotropy (CSA) (*8*). In contrast, carbon-13 chemical shift anisotropies have been reported for hundreds of compounds even though the ^{13}C chemical shift range is comparable to that of ^{27}Al (*9*). The Knight shift (*10*) is an anisotropic interaction which may influence the line shape of a solid-state ^{27}Al NMR spectrum in a fashion analogous to the anisotropic CS interaction; however, it is only operative in conducting and semiconducting materials. For example, the Knight shift has been shown to be important in solid-state ^{27}Al NMR spectra of binary aluminum–metal alloys (*11, 12*).

In this communication, solid-state ^{27}Al NMR spectra are presented for the crystalline 1:1 complex of $AlCl_3$ and $OPCl_3$, $AlCl_3 \cdot OPCl_3$ (**1**). Compound **1** and other analogous systems (Group 13 Lewis acids, phosphine oxide complexes) have been of interest for over 100 years (*13, 14*). Compound **1** is of particular interest, since the P–O–Al bond angle is close to 180° and the molecule has a near-C_{3v} symmetry. The effects of the ^{27}Al CSA, the nuclear quadrupole interaction and the relative orientation of the chemical shielding and electric field gradient (efg) tensors on the appearance of the ^{27}Al NMR spectra are discussed in detail. In addition, we present theoretical *ab initio* restricted Hartree–Fock (RHF) and density functional theory (DFT) calculations of the ^{27}Al chemical shifts and the electric field gradient at the aluminum nucleus.

DISCUSSION

Theoretical Background

The total internal NMR Hamiltonian for a spin-5/2 nucleus can be written as

$$\mathcal{H} = \mathcal{H}_Z + \mathcal{H}_Q + \mathcal{H}_{CS}. \quad [1]$$

For nuclei with relatively small quadrupole moments such as ^{27}Al, the quadrupolar and CS interactions can be treated as perturbations on the Zeeman Hamiltonian. In the solid state, chemical shielding is dependent upon the orientation of the molecule with respect to the external magnetic field. The chemical shielding interaction is described by a second-rank tensor, $\boldsymbol{\sigma}$, and can be expressed with the Hamiltonian

[1] To whom correspondence should be addressed. E-mail: rodw@is.dal.ca.

1090-7807/98 $25.00

$$\mathcal{H}_{CS} = \gamma h \mathbf{I} \cdot \boldsymbol{\sigma} \cdot \mathbf{B}_0 / 2\pi, \quad [2]$$

where $\mathbf{I}$ is the nuclear spin operator and $\mathbf{B}_0$ is the applied external magnetic field. The chemical shielding tensor has three principal components (σ_{ii}) which are assigned according to the following protocol, from least to most shielded: $\sigma_{11} \leq \sigma_{22} \leq \sigma_{33}$. In practice, *chemical shifts* are measured; that is, one can define a chemical shift tensor where the principal components are reported relative to some standard (e.g., for ^{27}Al, the standard is 1 M aqueous $Al(NO_3)_3$). The principal components of the chemical shift tensor are denoted, from least to most shielded, such that $\delta_{11} \geq \delta_{22} \geq \delta_{33}$ (*15*). The CS tensor can also be conveniently described with three parameters which correlate its principal components: the isotropic chemical shift, δ_{iso}, the span, $\Omega = \delta_{11} - \delta_{33}$; and the skew, $\kappa = 3(\delta_{22} - \delta_{iso})/\Omega$. The first two parameters are reported in ppm, while the latter is a dimensionless quantity describing the axiality of the spectrum with the limits $-1 \leq \kappa \leq +1$.

The quadrupolar Hamiltonian is written as

$$\mathcal{H}_Q = \frac{eQ}{2I(2I-1)\hbar} \mathbf{I} \cdot \mathbf{V} \cdot \mathbf{I}, \quad [3]$$

where Q is the nuclear quadrupole moment, I is the nuclear spin quantum number, $\mathbf{I}$ is the nuclear spin operator, and $\mathbf{V}$ is the electric field gradient tensor. The efg tensor is traceless and symmetric, and can be diagonalized in a suitable coordinate system. The diagonalized efg tensor has three principal components, which are assigned such that $|V_{zz}| \geq |V_{yy}| \geq |V_{xx}|$. The magnitude of the nuclear quadrupole interaction between the nuclear quadrupole moment and the efg is commonly described by the nuclear quadrupole coupling constant (NQCC or χ_Q) and the quadrupolar asymmetry parameter (η_Q) which are defined as $\chi_Q = e^2 q_{zz} Q/h$ and $\eta_Q = (V_{xx} - V_{yy})/V_{zz}$, respectively.

The NMR spectrum of a half-integer quadrupolar nucleus of spin I has a central transition ($+1/2 \leftrightarrow -1/2$) with $2I - 1$ satellite transitions. In this communication, we consider only the central transition, which is not affected by the first-order quadrupolar interaction (*16, 17*). For ^{27}Al, the NMR line shape of the central transition in a stationary powder sample is dependent upon χ_Q, η_Q, the principal components of the CS tensor, and the relative orientation of the CS and efg tensors. Simulation of the central transition is straightforward if the efg and CS tensors are coincident; however, this is most often not the case, and knowledge of the relative orientation of the efg and CS tensors is necessary. The relative orientation of the tensors is characterized by Euler angles α, β, and γ, which allow for unitary transformation between the two principal axis systems (PAS). Detailed descriptions of the relevant theory necessary for the simulation of such spectra are available elsewhere (*18*). Since the NMR spectrum of a quadrupolar nucleus is calculated in terms of the relative orientation of the quadrupolar interaction (QI) with respect to the laboratory frame, the convention used in this paper is to describe the chemical shift interaction within the PAS of the QI by the right-handed rotations

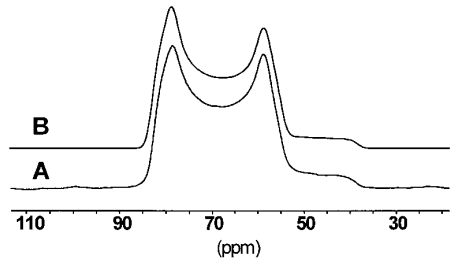

FIG. 1. (A) Solid-state ^{27}Al MAS NMR spectrum of $AlCl_3 \cdot OPCl_3$ obtained at 9.4 T with spinning speed $\nu_{rot} = 8$ kHz. (B) Simulated ^{27}Al MAS NMR spectrum (see text for parameters).

$$\boldsymbol{\delta}_{CS}^{QI} = \mathbf{R}_{Z''}(\gamma)\mathbf{R}_{Y'}(\beta)\mathbf{R}_{Z}(\alpha)\boldsymbol{\delta}_{CS}^{PAS}, \quad [4]$$

where $\boldsymbol{\delta}_{CS}$ are chemical shift tensors in the QI and CS PAS, respectively. Under conditions of rapid magic-angle spinning (MAS) the line shape of the central transition of a spin $n/2$ nucleus depends only upon χ_Q and η_Q. In addition, the position of the transition depends on δ_{iso} χ_Q and η_Q. Obtaining these parameters independently from the simulation of an MAS NMR spectrum greatly aid in the analysis of the NMR spectrum of the stationary sample.

Aluminum-27 MAS NMR

The solid-state ^{27}Al MAS NMR spectrum of the central transition of **1** obtained at 9.4 T is pictured in Fig. 1A. From an X-ray crystal structure of **1**, it was determined that the space group is $P2_1/m$ with $Z = 2$ (*19*). The molecules in the unit cell are crystallographically equivalent; therefore, the principal components of their CS and efg tensors are identical. The simulated spectrum (Fig. 1B) was obtained from the following parameters: $\delta_{iso}(^{27}Al) = 88(1)$ ppm, $\chi_Q(^{27}Al) = 6.0(1)$ MHz, and $\eta_Q = 0.15(1)$. The isotropic chemical shift is similar to other ^{27}Al shifts of $AlCl_3$ complexes measured in both the solution and solid state (*2, 20, 21*) and is in agreement with solution NMR data acquired for **1** (*14*). The quadrupolar asymmetry parameter and high molecular symmetry allow us to draw some qualified conclusions about the orientation of the efg tensor in the molecular frame. According to the X-ray crystal structure, the chlorine atoms bonded to the aluminum and phosphorus atoms are arranged in eclipsed conformations (all Cl–Al $\cdots$ P–Cl torsional angles are ca. 0.0°), and the complex has near-C_{3v} symmetry, since the Al–O–P bond angle is 176.0(4)°. There is a mirror plane parallel to the approximately linear Al–O–P axis containing two chlorine atoms, with the remaining chlorine atoms related by reflection through the mirror plane. If the Al–O–P bond angle was exactly 180°, the

local symmetry would dictate that $\eta_Q = 0$ with the largest component of the efg tensor being parallel to the Al–O bond. The small departure from linearity (4°) of the Al–O–P bond angle and the near axial symmetry of the efg tensor indicate that V_{zz} must be oriented near the Al–O bond axis.

Aluminum-27 NMR of the Stationary Sample

Experimental and calculated ^{27}Al NMR spectra of the central transition of a stationary sample of **1** are presented in Figs. 2A and 2B, respectively. In Fig. 2C, the stationary ^{27}Al NMR spectrum is simulated using the parameters obtained from the ^{27}Al MAS NMR spectrum with the assumption that the ^{27}Al CSA is zero. In comparing this calculated spectrum (2C) to the experimentally obtained spectrum (2A), the positions of the discontinuities and the overall width of the transition clearly indicate that there is an additional interaction determining the overall line shape of the powder pattern. Utilizing the quadrupolar parameters and isotropic chemical shift obtained from the simulation of the MAS NMR spectra, the calculated stationary spectrum (2B) is obtained from the additional parameters $\Omega =$ 60(1) ppm, $\kappa = -0.70(2)$, $\alpha = 90°$, $\beta = 90°$, and $\gamma = 0°$. This corresponds to ^{27}Al CS tensor principal components of $\delta_{11} =$ 125(1) ppm, $\delta_{22} = 74(1)$ ppm, and $\delta_{33} = 65(1)$ ppm.

The Euler angles reveal that the chemical shift tensor is oriented such that the least shielded component, δ_{11}, is parallel to the largest component of the efg tensor, V_{zz}, which must be along or close to the direction of the Al–O bond axis. The relative orientation of the other principal components of the two interaction frames is known (i.e., δ_{22} is parallel to V_{xx} and δ_{33} is parallel to V_{yy}). It is not possible to determine their orientations with respect to the molecular frame, other than to say that one set is perpendicular to the mirror plane in the molecule and the other set is parallel to this plane.

Second-moment analysis (*22*) reveals that the line broadening of the central transition results mainly from dipolar coupling of the aluminum nucleus with the three directly bonded chlorine nuclei and the phosphorus nucleus (from the X-ray structure the direct dipolar coupling constants are calculated to be $R_{DD}(^{27}\text{Al}, ^{35}\text{Cl}) = 330$ Hz and $R_{DD}(^{27}\text{Al}, ^{31}\text{P}) = 383$ Hz, respectively).

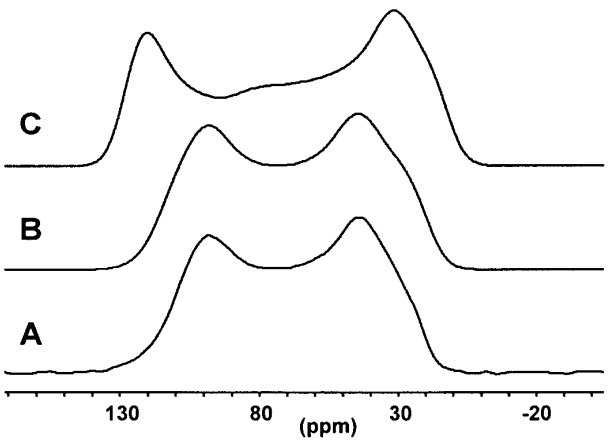

FIG. 2. (A) Solid-state ^{27}Al NMR spectrum of a stationary sample of $AlCl_3 \cdot OPCl_3$ at 9.4 T. (B) Simulation of the spectrum with CSA, $\Omega = 60$ ppm. (C) Simulation of the spectrum without CSA, $\Omega = 0$ ppm. See text for parameters.

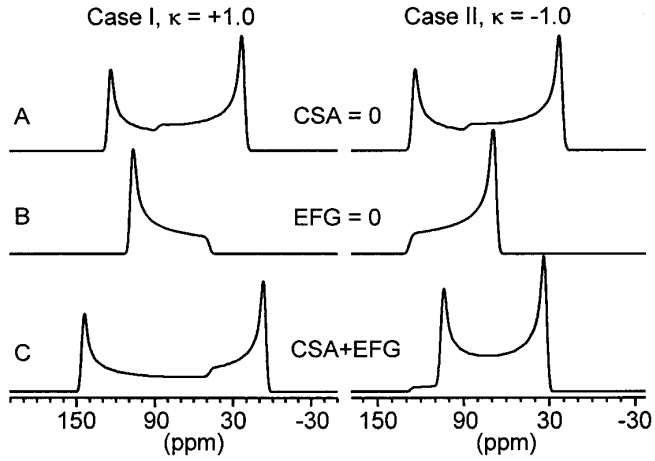

FIG. 3. The effects of (A) the quadrupole interaction, (B) CS anisotropy, and (C) combination of quadrupole interaction and CS anisotropy on the solid-state NMR spectrum of a quadrupolar nucleus. Case I, when CS ≠ 0, $\kappa = +1.0$. Case II, when CS ≠ 0, $\kappa = -1.0$. Parameters are $\chi_Q = 6.0$ MHz, $\eta_Q = 0.0$, $\delta_{iso} = 88$ ppm, $\Omega = 60$ ppm, $\beta = 0°$.

A calculated NMR spectrum of the central transition of a spin-5/2 nucleus in a stationary powder sample with an axially symmetric efg tensor and no chemical shift anisotropy is pictured in Fig. 3A (shown twice for comparison with the spectra below). The discontinuities in the spectrum correspond (moving from high to low frequency) to orientations in which the unique component of the efg tensor is perpendicular to ($\theta = 90°$), parallel to ($\theta = 0°$), and oriented at 41.8° with respect to the external magnetic field, $\mathbf{B}_0$. The isotropic chemical shift is not located at the center of gravity of the spectrum due to the second-order quadrupole shift (*17*).

To consider the effects of CSA on the appearance of an NMR spectrum of a spin-5/2 nucleus, first examine two NMR powder patterns of nuclei in which the CS and Zeeman interactions are the only interactions present (i.e., efg = 0). These simulated spectra are pictured in Fig. 3B. In Case I, $\delta_{11} = \delta_{22}$ (i.e., the unique component is δ_{33}) and the skew $\kappa = +1.0$. Discontinuities occur in this spectrum (from high to low frequency) at points at which the unique component of the CS tensor is perpendicular ($\vartheta = 90°$) and parallel ($\vartheta = 0°$) to the external magnetic field. In Case II, $\kappa = -1.0$ and δ_{11} is the unique component. Discontinuities occur at the same relative orientations of the unique CS tensor component and magnetic field; however, the parallel orientation is now at higher frequency than the perpendicular orientation. In both cases, the isotropic chemical shift occurs at the center of gravity of the spectrum, where $\vartheta = 54.74°$.

TABLE 1
Experimental and Calculated Aluminum-27 Chemical Shift Tensors in $AlCl_3 \cdot OPCl_3$[a]

Source	δ_{11} (ppm)	δ_{22} (ppm)	δ_{33} (ppm)	δ_{iso} (ppm)	Ω (ppm)[b]	κ[c]
Experimental[d]	125	74	65	88	60	−0.7
RHF[e]						
6-31G*	115.9	58.5	53.8	76.1	62.0	−0.85
6-31+G*	120.1	61.1	55.9	79.0	64.3	−0.84
6-311G*	162.5	93.6	87.6	114.6	74.9	−0.84
6-311+G*	161.3	92.8	86.9	113.7	74.4	−0.84
DFT(B3LYP)[e]						
6-31G*	142.6	81.6	77.0	100.4	65.6	−0.86
6-31+G*	148.6	79.4	73.6	100.5	75.0	−0.85
6-311G*	214.0	130.7	124.6	156.4	89.4	−0.86
6-311+G*	213.5	130.8	124.7	156.3	88.9	−0.86

[a] Geometry of $AlCl_3 \cdot OPCl_3$ taken from experimental X-ray crystal structure.
[b] Span of the CS tensor, $\Omega = \delta_{11} - \delta_{33}$.
[c] Skew of the CS tensor, $\kappa = 3(\delta_{22} - \delta_{iso})/\Omega$.
[d] Experimental chemical shifts referenced with respect to $Al(H_2O)_6^{3+}$(aq), $\delta(^{27}Al) = 0$ ppm.
[e] Theoretical chemical shifts referenced with respect to AlH_4^-, $\delta(^{27}Al) = 101$ ppm (see Experimental).

Finally, the combined effects of CSA and the quadrupolar interaction are pictured in Fig. 3C. If both quadrupolar interactions and CS interactions from Case I ($\kappa = +1.0$) are present, the breadth of the NMR spectrum of the quadrupolar nucleus increases. Conversely, if CS interactions from Case II are present ($\kappa = -1.0$), the breadth of the spectrum decreases. This information allows one to use simulated spectra to determine (i) if there is CS anisotropy in the NMR spectrum of the central transition of a quadrupolar nucleus and (ii) the skew of the CS tensor at the quadrupolar nucleus. This methodology was also applied to the results of Woessner and Timken, who reported a ^{27}Al NMR spectrum of a stationary sample of low albanite, but were unable to satisfactorily simulate the spectrum by considering the quadrupolar interaction alone (*23*). We performed spectral simulations which reveal that the spectral appearance is due to a small ^{27}Al CSA of 18(2) ppm and $\beta = 20(2)°$. The smaller CSA and χ_Q (3.37 MHz) relative to those observed in **1** are in accordance with the increased symmetry of a tetrahedrally coordinated AlO_4 center in albanite compared to the tetragonal $AlCl_3$ center in **1**.

Theoretical Calculations

The comparison of experimentally obtained chemical shift tensors and quadrupolar parameters to those calculated from first principles provides a means of testing the accuracy and validity of various computational schemes. There are excellent reviews in the literature which discuss the calculation of chemical shielding by Hartree–Fock and DFT methods (*24*) as well as publications which have made comparisons between the two methods (*25*). Theoretical calculations have been quite successful in predicting the orientation of CS tensors in the molecular frame (*26*). Recent work has focused on either first-row elements (*27*) or ^{31}P chemical shielding tensors (*28*). There have been very few reports of *ab initio* calculations of ^{27}Al CS parameters (*29–32*), and to our knowledge, no theoretical ^{27}Al CS tensors have been reported in the literature. The chemical shift tensor calculations presented in this paper serve several purposes. First, they allow for comparison between experimentally derived and theoretically calculated CS tensors. Second, the CS parameters resulting from calculations performed with RHF and DFT methods available under the Gaussian 94 platform are compared. DFT calculations were performed using the B3LYP exchange functionals (*33*). Third, the effects of basis set on the CS and efg tensor principal components are tabulated. Finally, theoretical CS and efg tensor orientations are obtained for comparison with those garnered from experiment.

A comparison of the experimental and theoretical ^{27}Al CS tensors is presented in Table 1. Experimental CS parameters are most closely predicted by the 6-31G* (RHF) and 6-31G* (B3LYP) calculations. Interestingly, all of the CS principal components become deshielded (most notably, δ_{11}) with the use of the larger triple-zeta basis set (6-311G*). The addition of diffuse functions (i.e., 6-31+G* and 6-311+G*) has little effect on the calculated results. The DFT calculations were completed in roughly two-thirds of the CPU time it took for analogous RHF calculations. In theory, the inclusion of electron correlation, which is implicit in DFT, should result in CS tensors which are closer to experimental results (*28*); however, this depends upon the form of the exchange correlational used in the calculation. Unfortunately, under the Gaussian 94 platform the DFT correlation functionals do not include magnetic field dependence, and this may help explain why DFT does not

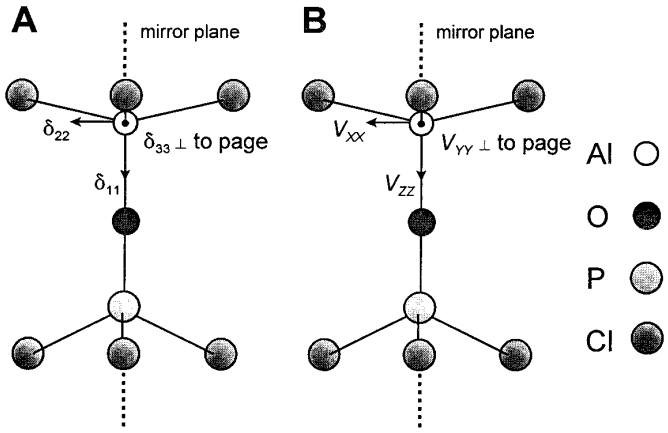

FIG. 4. (A) Theoretical orientation of the ^{27}Al CS tensor in the molecular frame. (B) Theoretical orientation of the efg tensor at the aluminum nucleus.

provide systematically better results than RHF calculations (*34*). The orientation of the ^{27}Al CS tensor is also obtained from the calculations and is pictured in Fig. 4A. RHF and DFT calculations predict almost identical tensor orientations regardless of basis set. The least shielded component of the CS tensor is oriented at 1.2° off of the direction of the Al–O bond vector, with δ_{33} contained within and δ_{22} perpendicular to the mirror plane. The theoretical orientation of δ_{11} is in agreement with the experimentally determined ^{27}Al CS tensor orientation.

The efg tensor was also calculated at the aluminum nucleus using several different basis sets (see Table 2). The conversion from atomic units (a.u.) to MHz is accomplished by multiplying the largest component of the efg tensor, V_{zz} by $eQ/h \times 9.7177 \times 10^{21}$ V m^{-2} (*35*). The values of χ_Q calculated by both RHF and DFT methods with 6-31G* and 6-31+G* basis sets are reasonably close to the experimental nuclear quadrupolar coupling constant, while larger basis sets overestimate its magnitude. The sign of χ_Q, which cannot be determined from the solid-state NMR experiments described here, is calculated to be negative. The quadrupolar asymmetry parameter is calculated as 0.11 or 0.12, in good agreement with the experimentally determined $\eta_Q = 0.15$, which is thought to be the result of the non-C_{3v} symmetry at the aluminum nucleus ($V_{xx} \neq V_{yy}$). The largest component of the efg tensor is oriented at 1.4° from the Al–O bond axis, with the remaining components perpendicular to this axis (as pictured in Fig. 4B). The theoretically calculated relative orientation of the CS and efg tensor is in exact agreement with our experimentally derived orientation, where the CS tensor is related to the fixed efg PAS by fixed rotations of $\alpha = 90°$ and $\beta = 90°$.

CONCLUSIONS

A definitive example of chemical shift anisotropy at the aluminum-27 nucleus has been presented. From solid-state ^{27}Al NMR spectra of spinning (MAS) and stationary samples of **1**, it was possible to obtain not only the *relative* orientation of the efg and CS tensors, but also the orientations of these tensors in the molecular frame. Our results demonstrate that tensorial NMR interactions provide invaluable information about the local symmetry about NMR-active nuclei and are very sensitive to slight changes in molecular structure. There is good agreement between theoretical and experimental CS and efg tensor parameters, but further work on related systems is warranted. Theoretically calculated orientations of interaction tensors are in agreement with experimental results; in particular, the unique components of each are predicted to be coincident. Comparison of the calculated CS tensors to experimental results shows that further modification of current computational schemes is needed in order to calculate chemical shift parameters for second-row elements accurately. The acquisi-

TABLE 2
Nuclear Quadrupole Parameters of the Aluminum Nucleus in $AlCl_3 \cdot OPCl_3$

Source	V_{zz} (a.u.)[a]	V_{yy} (a.u.)	V_{xx} (a.u.)	χ_Q (MHz)[b]	η_Q[c]
Experimental	—	—	—	6.0 (1)	0.15 (1)
RHF					
6-31G*	−0.2309	0.1287	0.1022	−7.60	0.11
6-311+G*	−0.2245	0.1258	0.0987	−7.39	0.12
6-311G*	−0.3026	0.1686	0.1339	−9.95	0.11
6-311+G*	−0.2957	0.1651	0.1306	−9.73	0.12
DFT					
6-31G*	−0.1983	0.1100	0.0883	−6.52	0.11
6-31+G*	−0.2135	0.1180	0.0956	−7.02	0.10
6-311G*	−0.2860	0.1582	0.1278	−9.41	0.11
6-311+G*	−0.2812	0.1558	0.1255	−9.25	0.11

[a] V_{ii} are principal components of the efg tensor, where $|V_{zz}| \geq |V_{yy}| \geq |V_{xx}|$.
[b] The largest component of the efg tensor, V_{zz}, is converted from atomic units to χ_Q in MHz by multiplying by 9.7177×10^{21} V m$^{-2} \times eQ/h$ (see text).
[c] Quadrupolar asymmetry parameter, $\eta_Q = (V_{xx} - V_{yy})/V_{zz}$.

tion and analysis of solid-state ^{27}Al NMR spectra of complexes which may also exhibit ^{27}Al CSA are currently in progress in our laboratory, since there is a large deficiency of information on anisotropic aluminum chemical shielding in the current literature.

EXPERIMENTAL

Solid-State NMR of $AlCl_3 \cdot OPCl_3$

The $AlCl_3 \cdot OPCl_3$ complex (**1**) was synthesized under an inert atmosphere by combining equimolar amounts of $OPCl_3$ and $AlCl_3$ in CH_2Cl_2, and recrystallizing from this same solvent (*19*). Solid-state aluminum-27 MAS NMR spectra and spectra of the stationary sample of **1** were acquired at $B_0 = 9.4$ T on a Bruker AMX-400 NMR spectrometer. Crystals of **1** were powdered and packed into 4mm and 7mm o.d. zirconium oxide rotors under an inert atmosphere. MAS spectra were acquired with spinning speeds between 2.5 and 8 kHz. Aluminum-27 chemical shifts were referenced with respect to $Al(H_2O)_6^{3+}(aq)$ ($\delta_{iso}(^{27}Al) = 0$ ppm) in a solution of 1 M $Al(NO_3)_3$ (aq). The aqueous standard was also used to determine the 90° pulse for ^{27}Al, which was set at 1.0 μs for the solid sample. Relaxation delays of 4 to 6 s were used with approximately 3400 and 9100 transients accumulated for MAS and static ^{27}Al spectra, respectively. Peaks were broadened by 100 Hz (MAS) and 400 Hz (stationary sample) with exponential multiplication of the FID. NMR spectra were simulated with the programs SECQUAD and WSOLIDS which were developed in this laboratory and incorporate the space-tiling method of Alderman and Grant as an efficient means of simulating solid-state NMR powder patterns (*36*).

Theoretical Calculations

Theoretical chemical shielding calculations were performed using the Gaussian 94 (*37*) suite of programs on an IBM RS6000/580 workstation. Gauge including atomic orbital (GIAO) (*38*) calculations of the ^{27}Al shielding tensors for **1** were performed using both restricted Hartree–Fock and density functional theory. The DFT calculations utilized the B3LYP exchange functionals (*33*). The molecular geometry of **1** used in these calculations was taken from a previously determined X-ray crystal structure (*19*). Calculated ^{27}Al chemical shifts were referenced with respect to AlH_4^-, since the absolute chemical shielding has been calculated as $\sigma_{iso}(^{27}Al) = 512$ ppm and the chemical shift of AlH_4^- is known with respect to the standard $Al(H_2O)_6^{3+}$, at $\delta_{iso}(^{27}Al) = 101$ ppm (*31, 39*). Gaussian 94 was also used to calculate the efg tensor at the aluminum nucleus.

ACKNOWLEDGMENTS

We thank Professor N. Burford for his interest and support of this research. We thank the Natural Sciences and Engineering Research Council (NSERC) of Canada (R.E.W.) for funding and the Atlantic Regional Magnetic Resonance Centre (ARMRC) for the solid-state NMR facilities. R.W.S. thanks the Killam Foundation and Walter C. Sumner Foundation for graduate fellowships. R.E.W. thanks the Canada Council for a Killam Research Fellowship. We are indebted to Dr. Klaus Eichele for the development of the WSOLIDS software used in our laboratory. We also thank Mr. Guy Bernard, Ms. Myrlene Gee, and Mr. Scott Kroeker for their many helpful comments and criticisms.

REFERENCES

1. T. J. Bastow, *Z. Naturforsch.* **49A,** 320–328 (1993).
2. J. W. Akitt, *Progr. Nucl. Magn. Reson. Spectrosc.* **21,** 1–149 (1989).
3. M. E. Smith, *Appl. Magn. Reson.* **4,** 1–64 (1993).
4. J. Klinowski, *Anal. Chim. Acta* **283,** 929–965 (1993).
5. L. B. Alemany, *Appl. Magn. Reson.* **4,** 179–201 (1993).
6. P. Pyykkö, *Z. Naturforsch.* **47A,** 189–196 (1992).
7. J. J. Delpuech, *in* ''NMR of Newly Accessible Nuclei—Volume 2: Chemically and Biochemically Important Elements'' (P. Laszlo, Ed.), pp. 153–195, Academic Press, New York (1983).
8. (a) A. Samoson, P. Sarv, J. P. v. Braam-Houckgeest, and B. Kraushaar-Czarnetzki, *Appl. Magn. Reson.* **4,** 171–178 (1993). (b) T. Vosegaard and H. J. Jakobsen, *J. Magn. Reson.* **128,** 135–137 (1997).
9. (a) T. M. Duncan, *in* ''Principal Components of Chemical Shift Tensors: A Compilation,'' 2nd ed., Farragut Press, Chicago, 1994. (b) T. M. Duncan, *J. Phys. Chem. Ref. Data* **16,** 125–151 (1987).
10. For a review on the Knight shift and references to original articles, see W. D. Knight and S. Kobayashi, *in* ''Encyclopedia of NMR'' (D. M. Grant and R. K. Harris, Eds.), pp. 2673–2679, Wiley, Chichester, England (1996).
11. M. E. Smith, M. A. Gibson, C. T. Forwood, and T. J. Bastow, *Philosoph. Mag. A* **74,** 791–809 (1996).
12. T. J. Bastow, M. E. Smith, and G. W. West, *J. Phys. Condens. Matter* **9,** 6085–6095 (1997).
13. See, for instance, (a) N. Burford, *Coord. Chem. Rev.* **112,** 1–18 (1992). (b) N. Burford, B. W. Royan, R. E. v. H. Spence, T. S. Cameron, A. Linden, and R. Rogers, *J. Chem. Soc. Dalton Trans., 1521–1528 (1990).*
14. F. Birkneder, R. W. Berg, and N. J. Bjerrum, *Acta Chem. Scand.* **47,** 344–357 (1993).
15. J. Mason, *Solid State Nucl. Magn. Reson.* **2,** 285–288 (1993).
16. K. Narita, J. Umeda, and H. Kusumoto, *J. Chem. Phys.* **44,** 2719–2723 (1966).
17. J. F. Baugher, P. C. Taylor, T. Oja, and P. J. Bray, *J. Chem. Phys.* **50,** 4914–4925 (1969).
18. (a) W. P. Power, R. E. Wasylishen, S. Mooibroek, B. A. Pettitt, and W. Danchura, *J. Phys. Chem.* **94,** 591–598 (1990). (b) J. T. Cheng, J. C. Edwards, and P. D. Ellis, *J. Phys. Chem.* **94,** 553–557 (1990).
19. N. Burford, A. Phillips, R. W. Schurko, R. E. Wasylishen, and J. F. Richardson, *J. Chem. Soc. Chem. Commun.* 2363–2364 (1998).
20. For $AlCl_3 \cdot$ tetrahydrofuran, the $\delta_{iso}(^{27}Al)$ is reported as 99 ppm from solid-state experiments. O. H. Han and E. Oldfield, *Inorg. Chem.* **29,** 3666–3669 (1990).
21. Several complexes of $AlCl_3$ and PMe_3 were investigated, with $\delta_{iso}(^{27}Al)$ of 111.5(2) and 54.3(2) ppm. P. J. Chu, A. de Mallmann, and J. H. Lunsford, *J. Phys. Chem.* **95,** 7362–7368 (1991).

22. J. H. Van Vleck, *Phys. Rev.* **74,** 1168–1183 (1948).

23. D. E. Woessner and H. K. C. Timken, *J. Magn. Reson.* **90,** 411–419 (1990).

24. See, for instance, A. C. de Dios, *J. Progr. Nucl. Magn. Reson. Spectrosc.* **29,** 229–278 (1996).

25. For example, see G. Rauhut, S. Puyear, K. Wolinski, and P. Pulay, *J. Phys. Chem.* **100,** 6310–6316 (1996).

26. Several articles on this subject can be found in ''Nuclear Magnetic Shieldings and Molecular Structure—NATO ASI Series C Vol. 386'' (J. A. Tossell, Ed.), Kluwer, Dordrecht (1993).

27. (a) M. Kaupp, O. L. Malkina, and V. G. Malkin, *J. Chem. Phys.* **106,** 9201–9212 (1997). (b) J. R. Cheeseman, G. W. Trucks, T. A. Keith, and M. J. Frisch, *J. Chem. Phys.* **104,** 5497–5509 (1996).

28. (a) D. B. Chesnut and E. F. C. Byrd, *Heteroatom Chem.* **7,** 307–312 (1996). (b) M. Kaupp, *Chem. Ber.* **129,** 535–544 (1996).

29. D. Sykes, J. D. Kubicki, and T. C. Farrar, *J. Phys. Chem. A* **101,** 2715–2722 (1997).

30. U. Schneider and R. Ahlrichs, *Chem. Phys. Lett.* **226,** 491–494 (1994).

31. J. Gauss, U. Schneider, R. Ahlrichs, C. Dohmeier, and H. Schnöckel, *J. Am. Chem. Soc.* **115,** 2402–2408 (1993).

32. M. Kanzaki, *J. Ceram. Soc. Jpn.* **105,** 91–92 (1997).

33. A. D. Becke, *J. Chem. Phys.* **98,** 5648–5652 (1993).

34. M. J. Frisch, A. Frisch, and J. B. Foresman, *in* ''Gaussian 94 User's Reference,'' pp. 109–110, Gaussian Inc., Pittsburgh (1996).

35. (a) R. D. Brown and M. P. Head-Gordon, *Mol. Phys.* **61,** 1183–1191 (1987). (b) P. L. Cummins, G. B. Bacskay, and N. S. Hush, *Mol. Phys.* **62,** 193–213 (1987).

36. D. W. Alderman, M. S. Solum, and D. M. Grant, *J. Chem. Phys.* **84,** 3717–3725 (1986).

37. M. J. Frisch, G. W. Trucks, H. B. Schlegel, P. M. W. Gill, B. G. Johnson, M. A. Robb, J. R. Cheeseman, T. A. Keith, G. A. Petersson, J. A. Montgomery, K. Raghavachari, M. A. Al-Laham, V. G. Zakrewski, J. V. Ortiz, J. B. Roresman, J. Cioslowski, B. B. Stefanow, A. Nanayakkara, M. Challacombe, C. Y. Peng, P. Y. Ayala, W. Chen, M. W. Wong, J. L. Andres, E. S. Replogle, R. Gomperts, R. L. Martin, D. J. Fox, J. S. Binkley, D. J. DeFrees, J. Baker, J. P. Stewart, M. Head-Gordon, C. Gonzalez, and J. A. Pople, ''GAUSSIAN 94'' (Revision B.2) (Gaussian, Inc., Pittsburgh, PA, 1995).

38. R. Ditchfield, *Mol. Phys.* **27,** 789–807 (1974).

39. H. Nöth, *Z. Naturforsch.* **35B,** 119–124 (1980).